Thermophysical and Tribological Properties of Highly Viscous Biolubricants

Xavier Paredes[1,2], José M. Liñeira del Río[1,3], David E.P. Gonçalves[3], María J.G Guimarey[1,4], María J.P. Comuñas[1,*], Jorge H.O. Seabra[5] and Josefa Fernández[1]

[1]Laboratory of Thermophysical and Tribological Properties, NaFoMat Group, Department of Applied Physics, Faculty of Physics and Institute of Materials (iMATUS), University of Santiago de Compostela, 15782, Santiago de Compostela, Spain.

[2]TERMOCAL Research Group, Research Institute on Bioeconomy, Escuela de Ingenierías Industriales, Universidad de Valladolid, Paseo del Cauce 59, Valladolid 47011, Spain.

[3]INEGI, Universidade do Porto, Faculdade de Engenharia, Rua Dr. Roberto Frias s/n, 4200-465 Porto, Portugal.

[4]Department of Design and Engineering, Faculty of Science & Technology, Bournemouth University, Talbot Campus, Poole, BH12 5BB, United Kingdom.

[5]FEUP, Universidade do Porto, Rua Dr. Roberto Frias s/n, 4200-465 Porto, Portugal.

*Corresponding author: María J.P. Comuñas

E-mail address: mariajp.comunas@usc.es

Abstract

Two new highly viscous biodegradable oils are investigated for use in wind turbine gearboxes (BIO-G00) and in mechanical transmissions of agricultural tractors (BIO-G02). Studies on their thermophysical and tribological properties were performed. High-pressure viscosity measurements were obtained up to 250 MPa and 363.15 K using a falling-body apparatus. The viscosity of BIO-G00 and BIO-G02 reaches maximum values of 14720 mPa and 7072 mPa. The film thickness and the tribological performance, from boundary to full-fluid lubrication regimes, under a slide-to-roll ratio of 5% obtained in a EHD2 ball-on-disc test rig are reported. Film thickness has also been computed through the Hamrock and Dowson equation, considering the inlet shear heating (thermal correction factor) due to the high viscosity of both biolubricants. Differences between the experimental and the theoretical film thickness are around 4% at 353.15 K and 14% at 303.15 K for both oils. The universal pressure-viscosity coefficients, α_{film}, for both oils are lower than those of other mineral and synthetic oils. Higher friction coefficients are obtained for BIO-G00 in all the studied lubrication regimes for the different rough discs and in the entire temperature range. A suitable wetting behavior on steel surfaces is observed for both selected oils.

Keywords

Sunflower base oils, high-pressure viscosity, viscosity-pressure coefficient; film thickness; Stribeck curves, wetting.

Introduction

The global market of lubricants was estimated at 40 millions of tons in 2017 [1]. While the advanced economies drop their consumption due to the use of improved lubricants and equipment, the demand from emerging countries grows every year [2]. Around half of these oils end up in the environment due to leaks or volatilization [3–5]. Better practices can be implemented to prevent leakages and disposal of used lubricants can also be improved [6]. However, the use of environmentally friendly fluids seems to be a more appealing alternative, especially when they can be obtained from natural sources [3,7–10]. Despite the advantages that the vegetable bases possess such as high viscosity index, high lubricity, low volatility and good boundary lubrication properties (their polar ester groups are able to adhere to metal surfaces), their low thermal stability, high pour point and low viscosity grade severely limit their widespread use [11]. Vegetable bases can be directly improved by chemical modification of the oil or genetic alteration of the plant, among others [7]. Formulations made from vegetable sources can be vastly improved by mixing them with other oil bases or by using suitable additive packages to combat oxidation, lower the pour point or improve their extreme pressure or antiwear properties, for example [12]. Anyway, considering the current social awareness on the matter, the final product should not only comply with a set of technical standards but also be as harmless as possible to the environment. To formulate vegetable oils that can compete with petroleum-based lubricants, extensive studies on their physicochemical and tribological properties are necessary [9]. In a previous work, the behavior at high pressures of lubricants based on high oleic sunflower oil for hydraulic applications was analyzed [13]. The original purpose was to formulate lubricants that met the European Ecolabel standard [14,15]. In the present work, two fully formulated oils based on high oleic sunflower oil (HOSO) are studied, BIO-G00 to be used in wind turbine gearboxes and BIO-G02 in mechanical transmissions of

agricultural tractors. In this kind of gearboxes, the operating temperature of the lubricant is around 343.15 K and pressures up to 2 GPa. The viscosity of the formulated mineral oil in use in these gearboxes (reference oil) was around 300 mPa·s at 313.15 K and 0.1 MPa, so the HOSO based oil was formulated with this viscosity value as target. While the physical properties at atmospheric pressure are easily measured, the viscosity at high pressure of such high viscous oils is difficult to obtain experimentally due to the lack of viscosity standards for high pressure-viscosity conditions. This article studies the viscosity behavior at high pressures, the pressure-viscosity coefficient, the ability to protect the moving mechanical solid surfaces that work under several load and speed conditions and the wettability (contact angles) of the lubricants with a steel surface.

Experimental Section

Materials

The fluids analyzed in this work (BIO-G00 and BIO-G02) are two newly formulated oils, which are based on high oleic sunflower oil (HOSO) with 83% of oleic acid. BIO-G00 has–25% of HOSO and BIO-G02 45%. These lubricants were formulated by Verkol Lubricantes, Navarra (Spain). The main characteristics (density and kinematic viscosity at 0.1 MPa and the viscosity index) of both formulated oils have been published in a previous work [16].

Experimental Techniques

The dynamic viscosity of the two formulated oils was measured from 288.15 K to 373.15 K with an expanded uncertainty of 1%, using a Anton Paar Stabinger SVM3000 rotational viscometer [17]. To find out if the behavior of vegetable oils is Newtonian, rheological tests were performed at 303.15 K using a rotational rheometer (Physica MCR 101, Anton

Paar), equipped with a cone-plate geometry with a cone diameter of 25 mm and a cone angle of 1°. The temperature is controlled with an uncertainty of 0.02 K with a Peltier P-PTD 200 device placed at the bottom plate. Viscosities at high pressure were measured using a falling body viscometer, VisLPT2, which can operate at pressures up to 280 MPa. This viscometer has been fully described in previous articles[13,18,19]. The viscometer cell, with a length of 425 mm, is formed by two concentric tubes and is covered by an aluminum frame where silicone oil is circulating. The total volume necessary to fill the viscometer cell is 70 cm^3. Two parallel electromagnetic coils (50 mm apart) are fixed to the outer tube, detecting the passage of a sinker through a variation of the magnetic flux (falling time of the sinker, Δt). We have used a cylindrical sinker with a hemispherical end, a nominal external diameter of 6.06 mm and a density of 7.441 g cm^{-3}. The sinker used had an axial through hole to reduce the falling times for high viscous samples. The viscometer body (cell and aluminum frame) is mounted in such a way that it can be rotated 180° to return the sinker to its initial position. To load a sample, in the viscometer cell a vacuum pump is used first to extract as much air as possible from the cell and pressure circuit tubes. When a low enough pressure is achieved, the valve connected to the vacuum pump is closed and the pump disconnected. The sample is then pressurized with a pneumatic pump.

One of the main difficulties encountered in this work is the calibration of the VisLPT2 viscometer, due to the high viscosity of the two biodegradable oils studied (BIO-G00 and BIO-G02). Literature viscosities for reference fluids of moderate viscosity that could be used to perform calibrations at high pressure have been published in the last decade[20–25]. For very high viscous fluids, as BIO-GOO and BIO-G02, whose viscosities at 0.1 MPa and 313.15 K are 228 and 137 , it has been proposed[25] to use as reference standard di(pentaerythritol) hexa(3,5,5-trimethylhexanoate), shortened as di*PE*i*C9* with

η(313.15 K, 0.1 MPa) =396.0 mPa s rather than less viscous reference standards as tris(2-ethylhexyl) trimellitate or squalane. Harris [24,26] measured the dynamic viscosity of diPE*i*C9 from 293.15 to 363.15 K and from 0.1 to 200 MPa, and Bair and Yamaguchi [27] from 323.15 to 363.15 K and from 62 to 700 MPa. Bair and Yamaguchi [27] have also reported a correlation based on the Yasutomi model of their viscosity values as well as those of Harris [24,26]. This correlation reproduces all viscosity values of diPE*i*C9 with a standard deviation of 3.7% at pressures up to 700 MPa. An aliquot of the DiPE*i*C9 sample studied by Harris and by Bair and Yamaguchi [27] was used.

The dynamic viscosity of the two formulated vegetable oils was obtained through the following expression:

$$\eta(p,T) = K(p,T)\left[\rho_{sinker}(T,p) - \rho(T,p)\right]\Delta t(p,T) \quad (1)$$

In this equation, ρ_{sinker} is the density of the sinker used in the falling body viscometer, VisLPT2. The density of the sample under study is ρ, $\Delta t(T,p)$ is the falling time and $K(p,T)$ is the calibration function. Applying this equation for DiPEiC9 we have:

$$\eta_{diPEiC9}(p,T) = K(p,T)[\rho_{sinker}(T,p) - \rho_{diPEiC9}(T,p)]\Delta t_{diPEiC9}(p,T) \quad (2)$$

Thus:

$$K(p,T) = \frac{\eta_{diPEiC9}(p,T)}{[\rho_{sinker}(T,p) - \rho_{diPEiC9}(T,p)]\Delta t_{diPEiC9}(p,T)} \quad (2)$$

and subsequently the viscosity of the vegetable oils can be obtained from:

$$\eta(p,T) = \frac{[\rho_{sinker}(T,p) - \rho(T,p)]}{[\rho_{sinker}(T,p) - \rho_{diPEiC9}(T,p)]} \frac{\Delta t(p,T)}{\Delta t_{diPEiC9}(p,T)} \eta_{diPEiC9}(p,T) \quad (3)$$

The density of the reference fluid DiPE*i*C9, $\rho_{diPEiC9}(T,p)$, was obtained from the Murnaghan EOS correlation reported by Bair and Yamaguchi [27] that reproduces the experimental relative volumes of DiPE*i*C9 with a standard deviation of 0.05%. Viscosity of the reference fluid DiPE*i*C9, $\eta_{diPEiC9}(T,p)$, needed in equation (3) was obtained from the correlation based on the Yasutomi model reported by Bair and Yamaguchi[27]. The

density of the formulated vegetable oils (BIO-G00 and BIO-G02), $\rho(T,p)$ were obtained from the correlations reported in a previous article[16]. It is worth mentioning that densities for BIO-G00 and BIO-G02 had to be extrapolated from 120 MPa (maximum pressure of Regueira et al.[16] density measurements) up to the pressures used in this work (up to 250 MPa). The uncertainty added to the viscosity measurements due to this extrapolation has been shown to be negligible compared to the uncertainties of other sources [18,28]. Considering the uncertainties of the temperature, pressure, falling times and those of the density and viscosity of the reference fluid an experimental uncertainty of 5% was estimated for the viscosity of the formulated vegetable oils (BIO-G00 and BIO-G02).

An EHD2 ball-on-disc tribometer was used to measure both the central film thickness, h_{exp}, and the friction coefficient, μ, at 303.15, 323.15 and 353.15 K under 50 N load. The contact generated by pressing the ball (carbon chrome steel) against the disc is under fully flooded lubrication (Figure 1). The tribometer is equipped with an optical interferometer to obtain the central film thickness by measuring the wavelength of the light that returns from the central plateau of the contact[29]. For film thickness measurements, a coated glass disc is used, while for friction coefficient measurements, three steel discs (100Cr6 AISI 52100) of different roughness (SD1, SD2 and SD3) were used. Several properties of the glass and discs were provided by the manufacturer and the average surface roughness (σ) was measured using a Hommelwerke Profiler (Table 1). The maximum Hertz pressure is 0.66 GPa for the film thickness measurements and 1.11 GPa for the friction coefficient tests.

The speeds of the disc (U_{disc}) and of the ball (U_{ball}) on the contacting surfaces at EHD2 apparatus are controlled by two electric motors for testing in rolling/sliding conditions. The average between the ball and disc speed is the entrainment speed (U_s). For every test the entrainment speed ramp used was 0.01 m s^{-1} to 2 m s^{-1}. These conditions

allow to work with very thin lubricant films (the precision of the EHD2 is 1 nm for lubricant films up to 1000 nm). For each test, the ball speed ranges from 0.097 to 1.950 m/s and the disc speed from 0.102 to 2.049 m/s. The slide-to-roll ratio (SRR) was determined through the equation:

$$SRR(\%) = 2\,\frac{|U_{disc}-U_{ball}|}{U_{disc}+U_{ball}}100 \qquad (4)$$

measurements were performed at a SRR of 5%. The obtained results for both, the central film thickness and the friction coefficient, are the average of two measurements at identical conditions. Although both oils are intended for use in applications where the contact is approximately linear, the conclusions drawn from these ball-on-disc tests should be qualitatively close to those obtained for a linear contact and therefore comparable. In the friction coefficient setup, the optical assembly is removed and the friction between the steel ball and the steel disc is measured with a torque cell on the ball shaft.

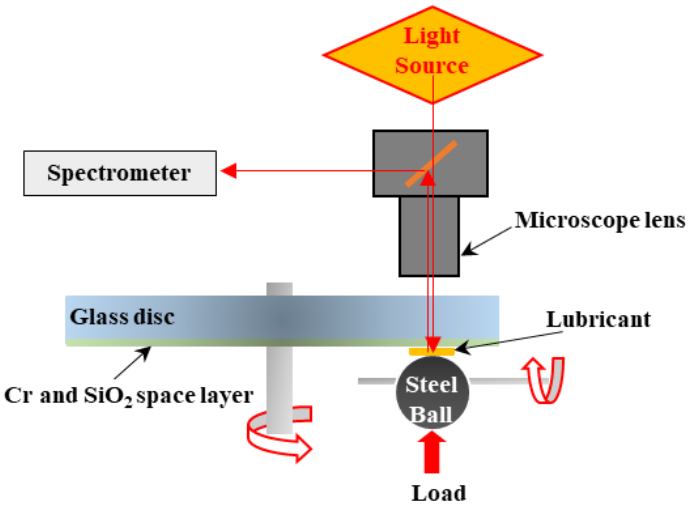

Figure 1. Scheme of EHD2 tribometer used for film thickness and friction coefficient measurements.

Contact angle, θ, of the two formulated biodegradable oils on steel surfaces was measured using the sessile drop method through a contact angle analyzer, Phoenix MT(A), at 303.15, 323.15 and 353.15 K. Figure 2 shows the experimental procedure used

for the contact angle measurements. The experimental setup was further described previously [30,31]. The same surface material of the disks used for the tribological tests was also selected to evaluate the wettability behavior (chrome steel discs AISI 52100). The surface was rinsed with ethanol and dried with a stream of hot air, before each measurement. One drop of lubricant sample was dropped on the steel surface using a syringe. The dynamic advancing contact angle (θ_A) was evaluated from pictures taken every second for 60 s. The average value of at least 4 measurements at each temperature is reported in this work.

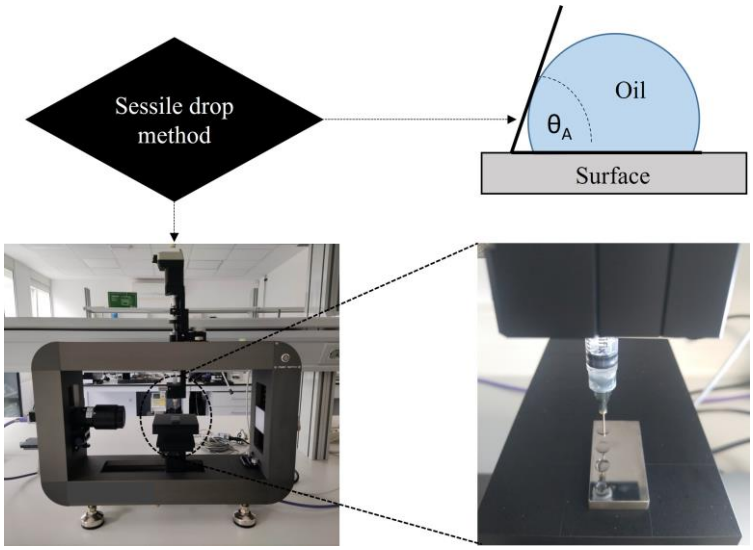

Figure 2. Experimental apparatus used for contact angle determination.

Results and discussion

The viscosity data at 0.1 MPa for BIO-G00 and BIO-G02 are reported in Table 2. The values have been compared with those published previously by Regueira et al. [16] obtaining excellent agreement. Thus, average absolute deviations of 0.8% and 0.2 % were obtained for BIO-G00 and BIO-G02, respectively. Figure 3 shows that both oils have high viscosities at atmospheric pressure, BIO-G00 being more viscous (gearboxes of wind turbines applications) than BIO-G02 lubricant (transmissions in agricultural tractors applications). At 0.1 MPa and over the complete temperature interval (288.15-373.15) K,

the viscosity of BIO-G00 ranges from 26 to 1018 mPa s and that of BIO-G02 from 19 to 544 mPa s. In addition, the change of the viscosity with temperature is lower for BIO-G02 accordingly with its higher viscosity index [16], VI=158 for BIO-G00 and VI= 166 for BIO-G02. Flow curves for BIO-G00 and BIO-G02 obtained with the rotational rheometer (Physica MCR 101, Anton Paar) are plotted in Figure 4, where it is shown that the shear stress is linear with the shear strain rate for both oils entailing Newtonian behavior at these conditions.

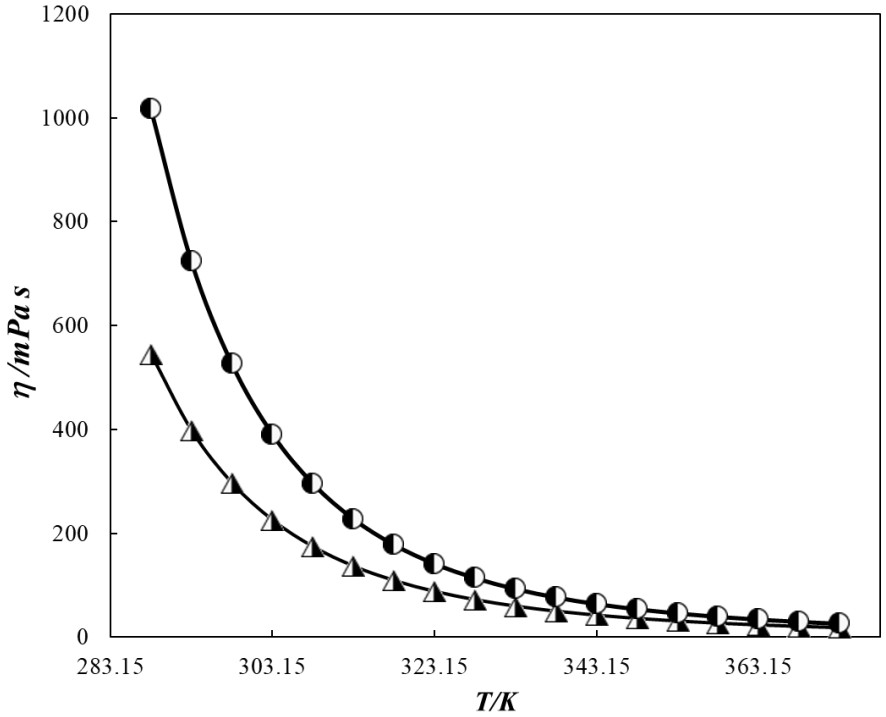

Figure 3. Temperature dependence of the viscosity at atmospheric pressure for the two formulated biodegradable lubricants: (◐) BIO-G00, (◭) BIO-G02 and (—) equation (6).

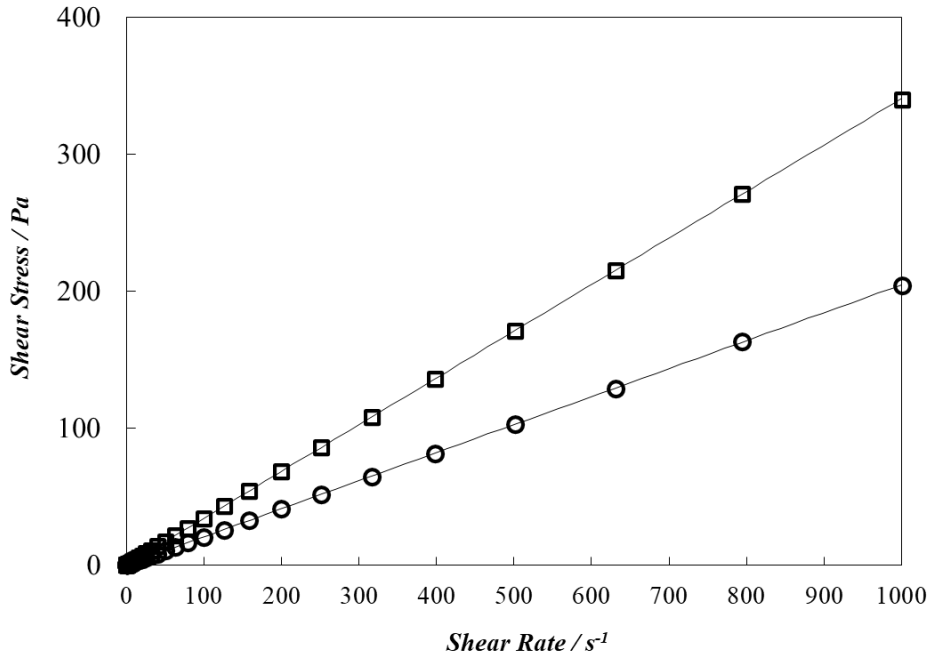

Figure 4. Flow curves for the both vegetable oils at 303.15 K: (□) BIO-G00 and (○) BIO-G02.

In this work, the falling times were measured for DiPEiC9, BIO-G00 and BIO-G02 at three temperatures 313.15, 343.15 and 363.15 K and at pressures up to 250 MPa. The falling times range from 21 s to 13966 s. Subsequently, using equation 3 and the procedure detailed above, the dynamic viscosity values reported in Table 3 for BIO-G00 and BIO-G02 were obtained. Figure 5 shows the pressure dependence of the viscosity for the two formulated vegetable oils for the three isotherms, being similar for both vegetable lubricants. Thus, at 313.15 K the viscosity at 250 MPa is around 58 times larger than the viscosity at 0.1 MPa for BIO-G00, and 39 times bigger for BIO-G02.

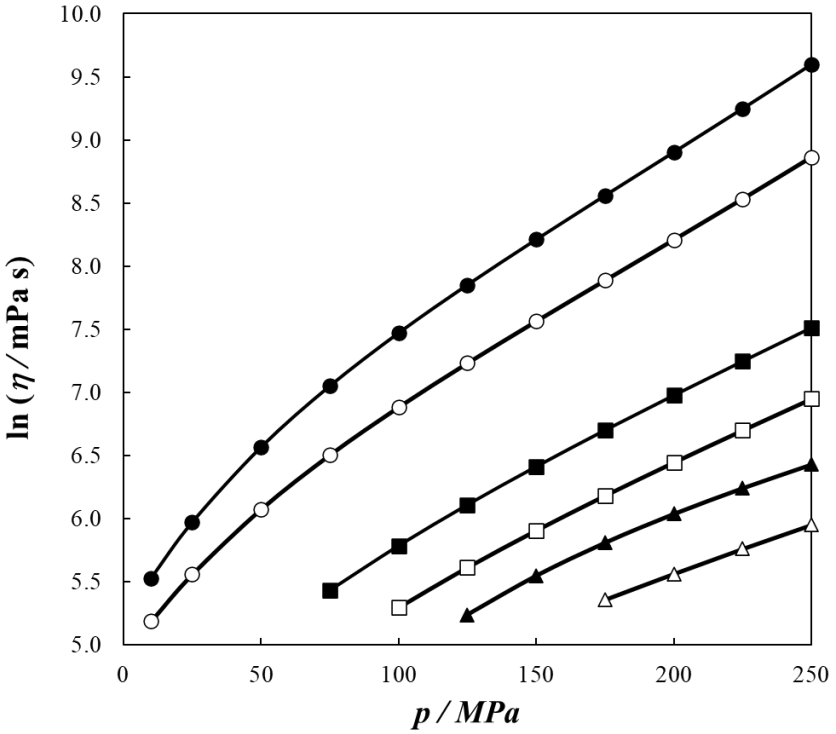

Figure 5. Dynamic viscosity (ln η) versus pressure at (●) 313.15 K, (■) 343.15 K and (▲) 363.15 K for the formulated vegetable lubricants: (black symbols) BIO-G00 and (white symbols) BIO-G02.

The pressure-viscosity coefficient (α) is another important property in elastohydrodynamic lubrication [32–34]. In this work, this coefficient has been obtained with the method proposed by Bair et al [34] from dynamic viscosity measurements at high pressures. For this purpose, the viscosity values of both formulated lubricants (Tables 2 and 3) were correlated using the following equation [35]:

$$\eta\,(T,p) = \eta_0\,(T)\,\left(\frac{p+E_0+E_1T+E_2T^2}{0.1MPa+E_0+E_1T+E_2T^2}\right)^D \qquad (5)$$

where:

$$\eta_0\,(T) = A\,exp\left(\frac{B}{T-C}\right) \qquad (6)$$

The parameters A, B and C have been determined in a preliminary fit of the viscosity as a function of the temperature at atmospheric pressure, η_0 (T), and the coefficients D, E_0, E_1 and E_2 have been fitted to the viscosity measurements at high pressures. The parameter

values are given in Table 4. Equation 5 reproduces the experimental dynamic viscosity values with average absolute deviation of 3.0% for BIO-G00 and of 2.7% for BIO-G02. Both values are lower than the estimated expanded uncertainty. From this correlation, the universal pressure-viscosity coefficient (α_{film}) and the reciprocal asymptotic isoviscous pressure coefficient (α^*) [34] were obtained as in previous works [36–38]. Table 5 reports the values of α_{film} and α^* at different temperatures for the two formulated vegetable oils. The α_{film} values are slightly higher for BIO-G00 than for BIO-G02. As expected, both coefficients decrease with temperature. The α_{film} values obtained in this work for both biodegradable lubricants were compared with other mineral reference oils used in wind turbines gearboxes, MIN-G01 and in transmission for agricultural tractors, MIN-G02[39]. As Figure 6 shows, the universal pressure-viscosity coefficients for BIO-G00 and BIO-G02 are lower than those of the reference oils which means that they are better at reducing friction, subsurface stresses, and pressure spikes[40]. The sequence for α_{film} is the same as that of the dynamic viscosities at 313.15 K and 0.1 MPa: BIO-G02 (137 mPa s) < MIN-G02 (161 mPa s[16,39]) for transmission oils, and BIO-G00 (228 mPa s) < MIN-G01 (283 mPa s[16,39]) for wind turbine oils. Considering that the film thickness is a function of both the pressure-viscosity coefficient and the viscosity at atmospheric pressure[13,19], the reference oils will generate a thicker lubricant film than the biodegradable oils. However, it is interesting to carry out experimental tests to determine the thickness of the protective layer and the friction coefficient, to know if the developed oils generate a film thick enough to adequately protect the surfaces. If so, the reference mineral oils could be generating a thicker film than necessary and therefore reducing the energy efficiency of the machinery in which they are used.

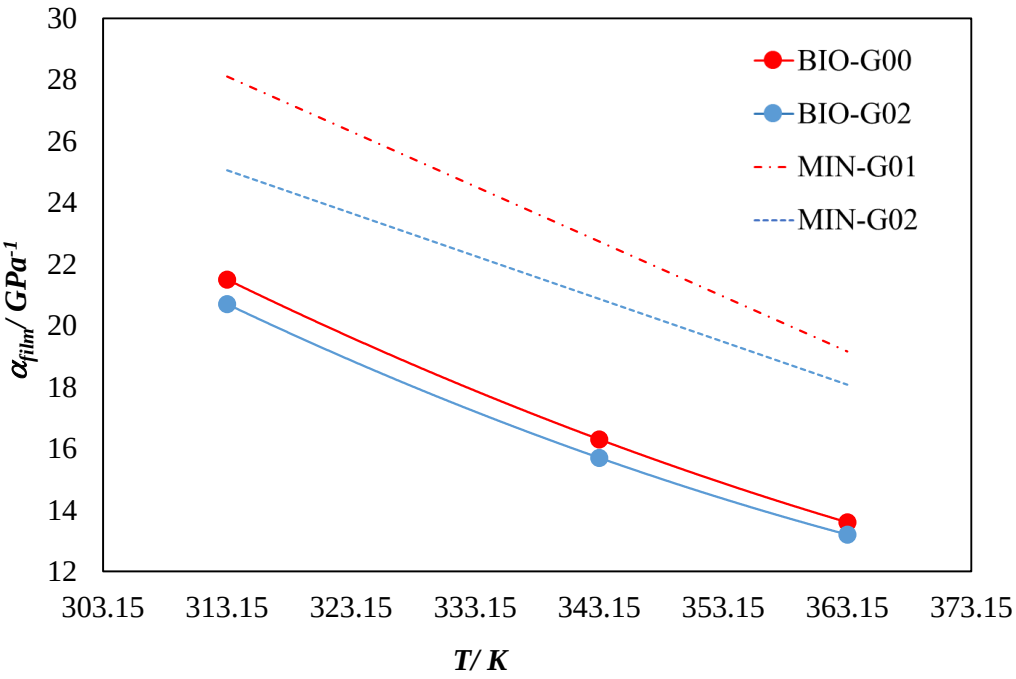

Figure 6. Universal pressure-viscosity coefficient (α_{film}) for the biodegradable lubricants studied in this work and for the reference oils[39] used in wind turbine (red color) and transmission in agricultural tractors (blue color).

The central film thickness values obtained with the EHD2 apparatus for steel-glass contact, h_{exp}, are illustrated in Figure 7 versus the entrainment speed, U_s, at different temperatures. As usual, the higher is the entrainment speed, the thicker is the film. For the BIO-G00 biodegradable oil, higher film thickness values were obtained in comparison with those obtained for BIO-G02, due to its much higher viscosity. On the other hand, film thickness of both lubricants decreases when temperature rises. Thus, for BIO-G00, h_{exp} ranges from 137 nm to 132 nm over all the entrainment speeds at 303.15 K, and from 37 to 378 nm at 353.15 K whereas for BIO-G02 the h_{exp} values range respectively from 97 to 1221 nm, and 23 to 285 nm. It should be noted that the precision of the interferometry method decreases when the film thickness is higher than 1000 nm.

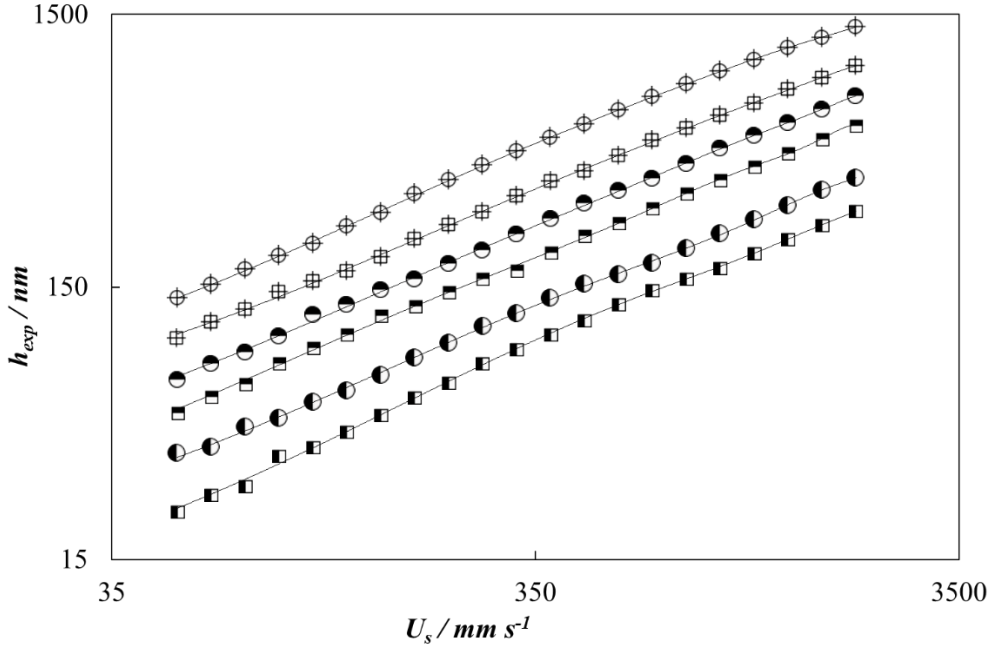

Figure 7. Experimental central film thickness for steel-glass contact, h_{exp}, of the studied biodegradable oils against the entrainment speed U_s: (⊕, ⊞) 303.15 K; (◓, ⬒) 323.15 K and (◐, ◧) 353.15 K. Circle symbols are used for BIO-G00 and square symbols for BIO-G02.

The experimental film thickness obtained with EHD2 apparatus, h_{exp}, has been compared with the predicted film thickness, h_{HD}, calculated from the Hamrock and Dowson equation (HD) [41]:

$$h_{HD} = 2.69 R_X \left(\frac{\eta_0 U_S}{E^* R_X}\right)^{0.67} (\alpha E^*)^{0.53} \left(\frac{F_N}{E^* R_X^2}\right)^{-0.067} \left[1 - 0.61 e^{\left(-0.73\left(1.03 \frac{R_y}{R_x}^{0.64}\right)\right)}\right] \quad (7)$$

where R_X is the equivalent radius in rolling direction, η_0 is the dynamic viscosity at test temperature and atmospheric pressure, E^* is the equivalent Young modulus of the specimens, U_S is the entrainment speed, F_N is the normal load, R_y is the equivalent radius perpendicular to the rolling direction, and α the pressure–viscosity coefficient at the test

temperature. The values of $\alpha*$ obtained from the high-pressure viscosity measurements, were used in this work in equation 7 to obtain the predicted film thickness h_{HD} [42]. As Figure 8 shows, remarkable differences are observed between the experimental and the predicted film thickness obtained through equation 7 for BIO-G00 and BIO-G02. At the highest temperature (lowest viscosity), the predicted film thickness obtained through equation 7 is closer to the experimental one, than that obtained at the lower temperature (higher viscosity). Such difference is attributed to a phenomenon previously reported in the literature[43], the inlet shear heating. This happens particularly at low temperatures (high viscosity) but also high speeds or high SRR. Since not all the lubricant can enter the contact, there is a lot of oil which stays outside and gets sheared considerably at the contact inlet. This shearing increases the temperature in this region and hence, reduces the viscosity of the lubricant and the effective film thickness. Therefore, it is necessary to consider the thermal effect correction (Φ_T) on the film thickness expression (equation 7). The following equation proposed by Gupta et al. [43] based on the articles of Cheng [44] and Wilson and Sheu [45] was used:

$$\Phi_T = \frac{1-13.2\ (p_0/E)\ L^{0.42}}{1+0.213\ (1+2.23SRR^{0.83})\ \ L^{0.640}} \tag{8}$$

In equation 8, p_0 is the maximum Hertzian pressure (0.66 GPa as has been indicated in the section of experimental techniques) and L is a thermal loading parameter calculated through the following expression:

$$L = \left(-\frac{d\eta_0}{dT}\right)\frac{{U_s}^2}{\kappa_f} \tag{9}$$

where κ_f is the thermal conductivity of the oils. As can be observed in the literature [46,47], the thermal conductivity of vegetable oils usually ranges from 0.16 to 0.17 $W{\cdot}m^{-1}{\cdot}K^{-1}$, besides it changes very little with the temperature. The thermal conductivity of both oils

was measured by using a hot wire Tempos-Meter Group conductivity meter with a KS-3 probe. The values obtained at 298.15 K are 0.159 $W \cdot m^{-1} \cdot K^{-1}$ for BIO-G00 and 0.155 $W \cdot m^{-1} \cdot K^{-1}$ for BIO-G02. These values were used for the calculation of thermal loading parameter, *L* using equation 9.

The derivative of the dynamic viscosity at atmospheric pressure with respect to the temperature, also needed in equation 9, has been determined through equation (6) as follows:

$$\frac{d\eta_0}{dT} = \frac{-AB}{(T-C)^2} exp\left(\frac{B}{T-C}\right) \quad (10)$$

where the values of A, B and C are reported in Table 4 for each oil. Finally, the film thickness values, once considered the thermal effect correction, h_{THD}, are calculated by using the following equation:

$$h_{THD} = \Phi_T \, h_{HD} \quad (11)$$

where h_{HD} is the film thickness value obtained with equation 7, without the inlet shear heating correction, from the Hamrock and Dowson [41] equation. As Figure 8 shows, the theoretical film thickness obtained considering the thermal correction, h_{THD}, is much closer to the experimental values h_{exp} determined with EHD2 apparatus for both formulated biodegradable oils. Once again, the best results are found for the higher temperature for which differences between h_{THD} and h_{exp} values are around 4%.

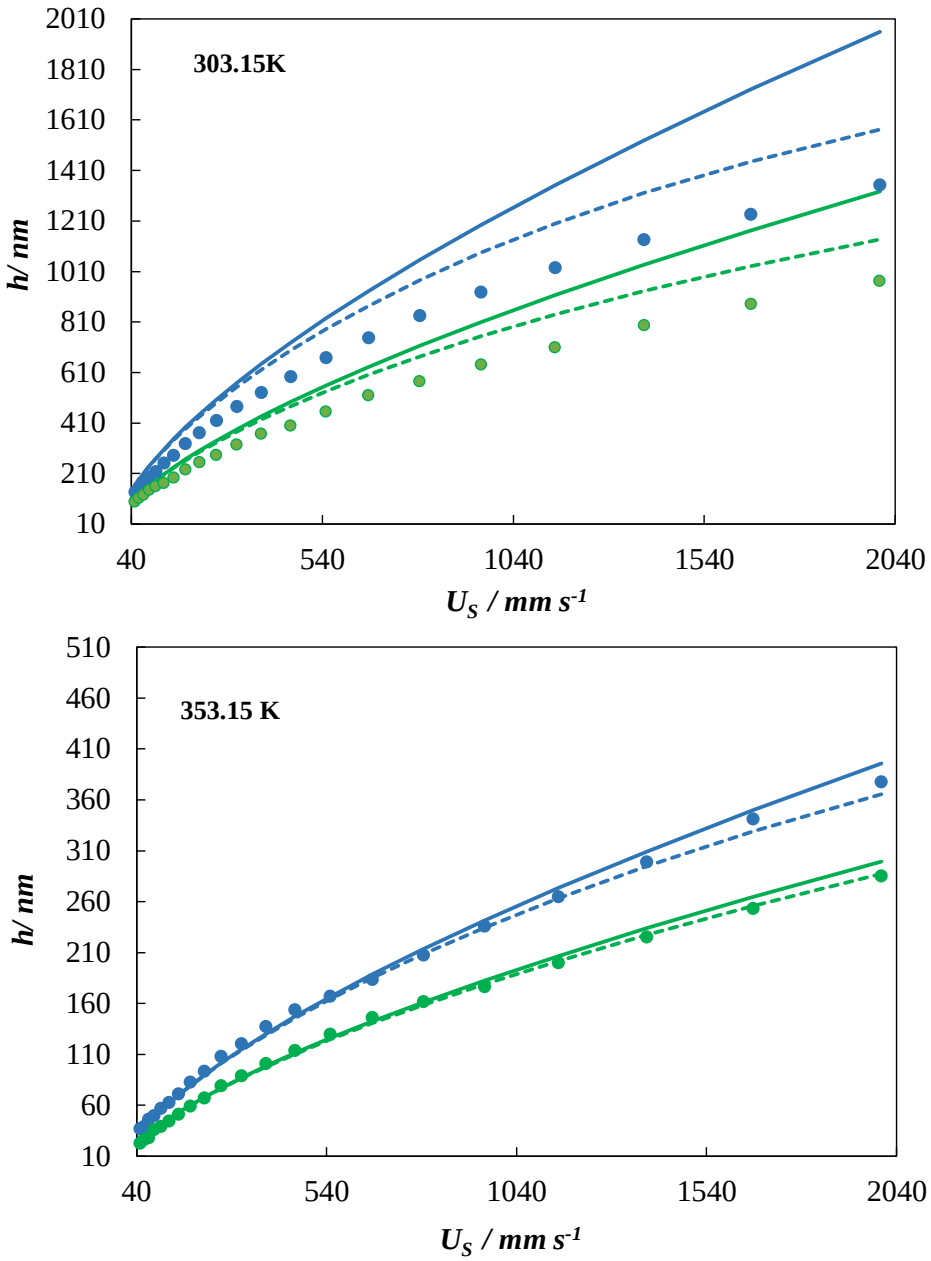

Figure 8. Film thickness against the entrainment speed. Experimental for steel-glass contact (h_{exp}, ●), theoretical film thickness without thermal correction, (h_{HD}, −), and theoretical film thickness with thermal correction (h_{THD} , ·····). Blue color is used for BIO-G00 and green color for BIO-G02.

Friction behavior of each lubricant was studied at three different temperatures (303.15, 323.15 and 353.15 K) and for a SRR value of 5%, through the Stribeck curves[48]. Friction is usually evaluated in terms of the friction coefficient, which depends on the conditions in which the interaction between the rubbing surfaces occurs: lubricant

viscosity (η), normal load (N), and sliding relative speed (v). The Stribeck curve relates the friction coefficient to the Hersey number, which is a dimensionless parameter involving these relevant physical parameters, $H= (\eta\ v)/N$, or to the film thickness expressed in a reduced form. To better understand the behavior of these curves, it is necessary to plot each one with its own abscissa, considering the film thickness obtained in each test and the different roughness of each disc, through the specific film thickness (Λ):

$$\Lambda = \frac{h_{sg}}{\sqrt{\sigma_{disc}^2+\sigma_{ball}^2}} \left(\frac{E_{sg}}{E_{ss}}\right)^{0.073} \quad (12)$$

where h_{sg}, is film thickness measured with a steel ball on glass disc contact, σ_{disc} *and* σ_{disc} are the surface roughness of the disc and the ball, and E_{sg} and E_{ss} are the elastic modulus for the steel-glass contact and the steel-steel contact respectively[49]. A full Stribeck curve was obtained for the two biodegradable oils: boundary to mixed (for SD3 and SD2 discs) and full film lubrication (SD2 and SD1 discs) as shown Figure 9. As expected, friction tests performed with rough discs produced higher friction values than those obtained with the smoothest disc. At all operating temperatures, BIO-00 presents higher coefficients of friction compared to those of BIO-G02 oil. This is especially true for the smooth discs (SD1 and SD2) and higher speeds for which the lubrication regime is between mixed and full-film (Λ>1). The higher friction values are due to the fact that the viscosity and the pressure-viscosity coefficient of the BIO-G00 are greater than those of BIO-G02. When Λ<1, the difference in the friction coefficient of both lubricants decreases as the boundary lubrication regime approaches and the dependence on the physical properties of the lubricant is much smaller, as expected.

Since those gears generally operate in the mixed lubrication regime where friction depends on the viscosity and pressure-viscosity coefficient, the friction coefficient of

vegetable oils should also be lower than that of the reference oils, assuming that the formers are both able to separate the surfaces effectively.

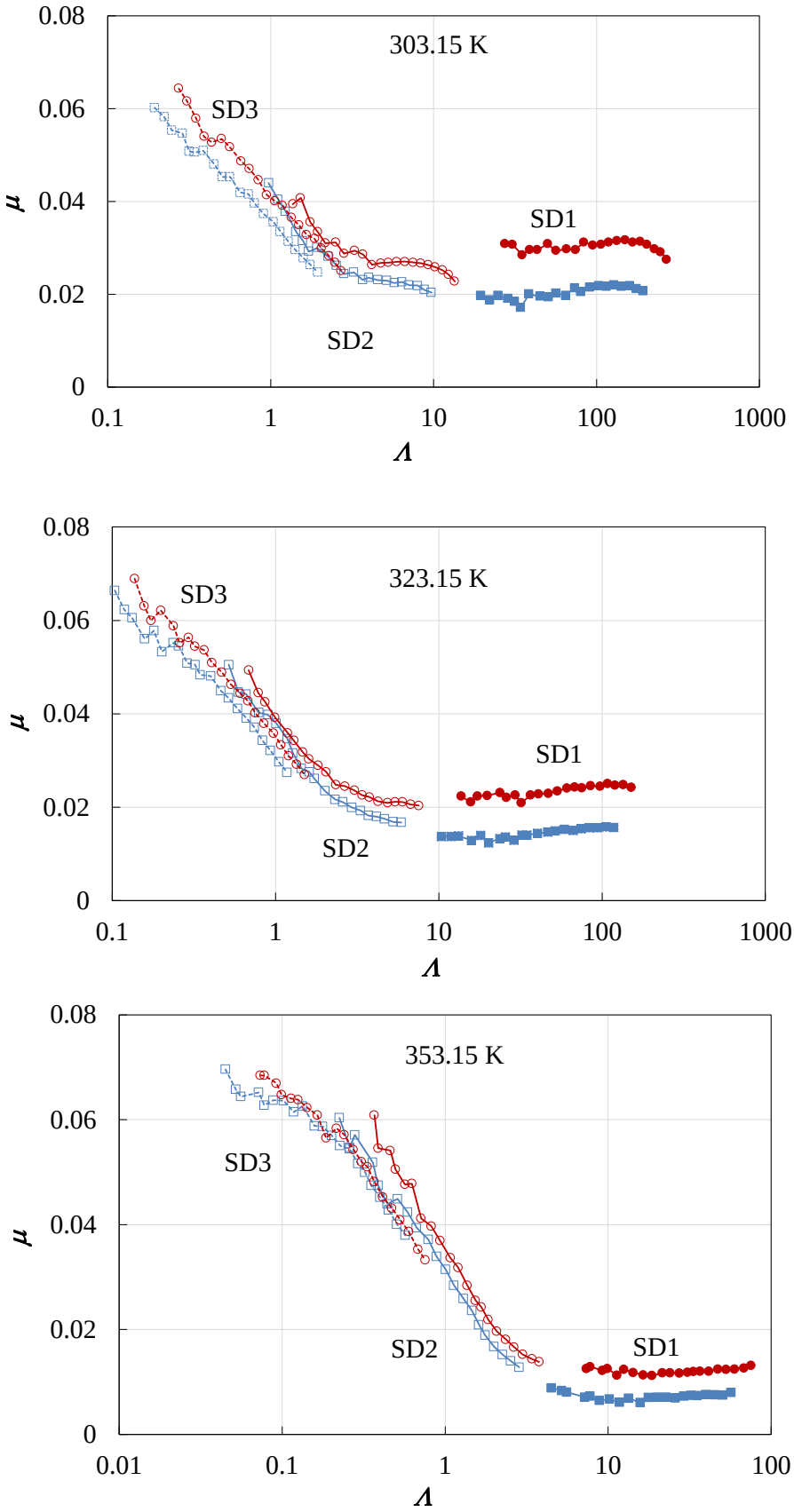

Figure 9. Stribeck curves at 5% SRR for rough and polished discs (SD3-SD1) for BIO-G00 (red color) and BIO-G02 (blue color) lubricants.

Finally, the wettability behavior of both vegetable oils on a steel surface was studied. The contact angle of the lubricant changes when it is deposited on the surface and requires a certain time to reach a stable value. Therefore, the evolution of the contact angle, θ, was recorded for 60 seconds as shown in Figure 10. As can be seen in this figure the steady state was reached for both oils (BIO-G00 and BIO-G02) at all temperatures in around 30 seconds. The difference between the contact angle of the two oils was greater at the lower temperature. BIO-G00 oil has a higher contact angle than BIO-G02 at 303.15 K, which suggests a poorer wetting of the former. However, this fact changes for the upper temperatures (323.15 and 353.15 K), the contact angle for BIO-G00 being smaller than for BIO-G02.

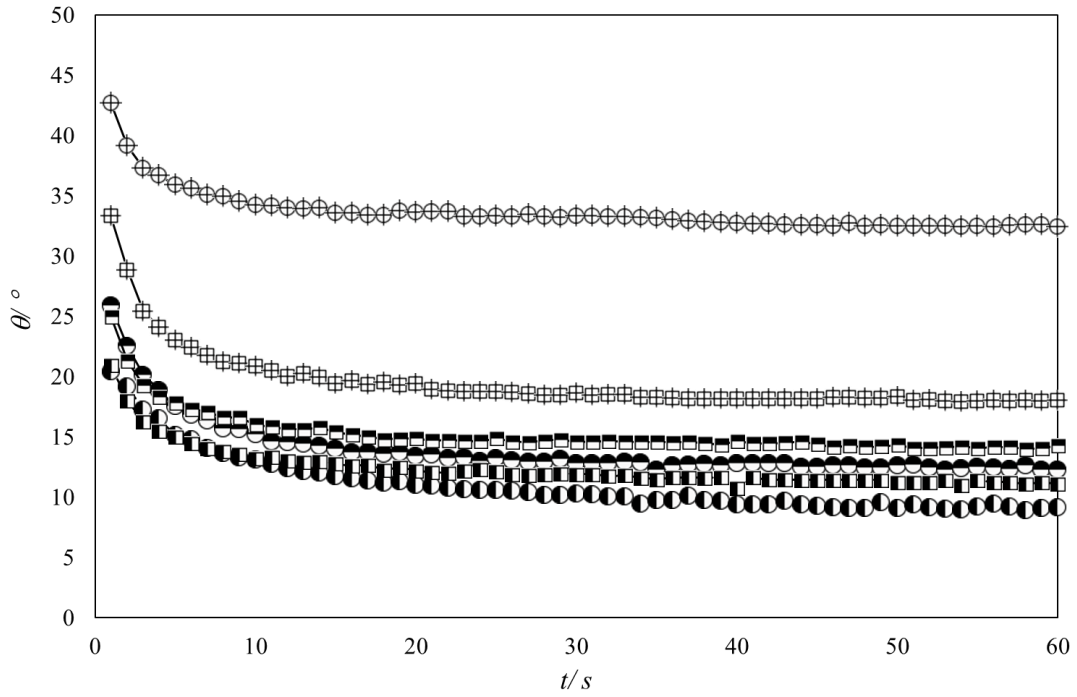

Figure 10. Temporal evolution of the contact angle, θ, of the formulated biodegradable oils on 100Cr6 steel surface: (⊕, ⊞) 303.15 K; (◓, ⬒) 323.15 K and (◐, ◧) 353.15 K. Circle symbols are used for BIO-G00 and square symbols for BIO-G02.

The average stationary contact angle and its standard deviation for each lubricant on 100Cr6/AISI 52100 steel at three different temperatures was collected in Table 6. As expected, the contact angle decreases as the temperature rises. The contact angle of a

lubricant depends on its viscosity, which means that for the higher viscosity the contact angle of the lubricant with the surface increases [50,51]. Viscosity is clearly higher for BIO-G00 than for BIO-G02, especially at low temperatures (Figure 3). The evolution of the advancing contact angle at the three temperatures for each biodegradable oil can be seen clearly in Figure 11, the images of the droplets were captured at 0, 30 and 60 s. The decrease in the contact angle is more pronounced as the temperature increases.

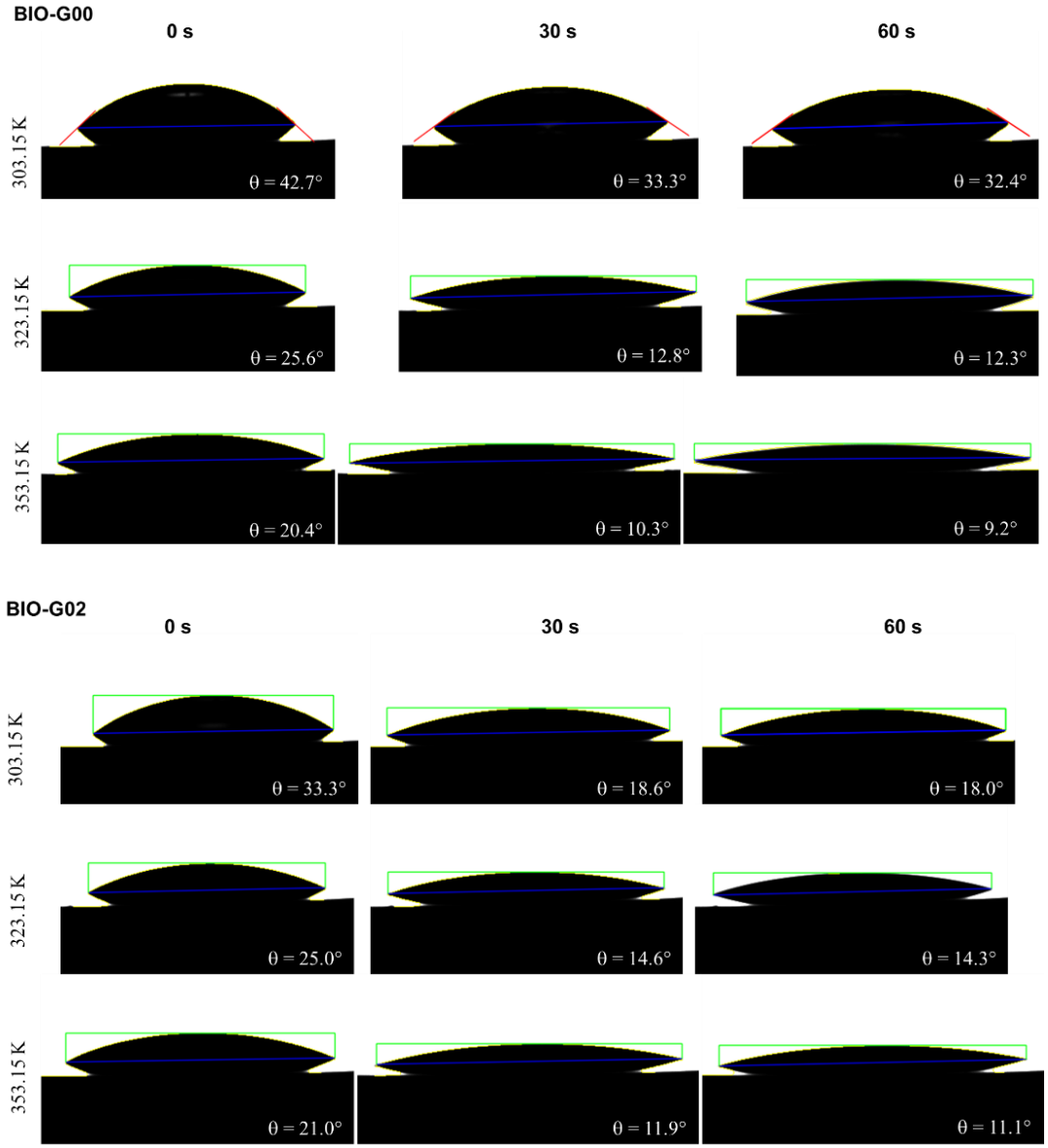

Figure 11. Drop images for BIO-G00 and BIO-G02 at 0, 30 and 60 s and at different temperatures.

In fact, the largest variation in contact angle for the same evolution time was observed for BIO-G00 at 353.15 K with a decrease of 55 % (from 20.4 to 9.2°). All contact angle values vary between 42.7° and 9.2°, showing a proper wetting behavior on steel surface for both selected oils.

Conclusions

Several lubricant properties of two high viscous formulated vegetable lubricants, which can achieve significant environmental benefits over the currently used mineral and synthetic oils, have been studied. The following features were achieved:

- Using reliable viscosity data of the high viscous di(pentaerythritol) hexa(3,5,5-trimethylhexanoate) ester to perform the calibration of the falling body viscometer, very viscous lubricants such as BIO-G00 and BIO-G02 at high pressure can be measured.
- The pressure effect on the dynamic viscosity is very significant for both oils reaching, over the 313.15 K isotherm, viscosity values around (40-60) times higher at 250 MPa than at 0.1 MPa.
- The variation in the experimental central film thickness, over the entrainment speeds range (40-2040 mm s^{-1}), is around 10% for BIO-G00 and 12 % for BIO-G02 at all the temperatures.
- Due to the inlet shear heating it is observed that the prediction of the film thickness for such viscous lubricants improves when the thermal effect correction is used in the Hamrock and Dowson equation for both biodegradable oils.
- Stribeck curves show low friction coefficients for both oils. Although the pressure-viscosity coefficient for the reference oils is higher and hence can produce a thicker film, the biodegradable oils studied must generate a thick film enough to adequately protect the surfaces, while still providing low friction, making them a suitable replacement.

- For high temperatures BIO-G02 and BIO-G00 show a similar wettability behavior.

Acknowledgments

Spanish Ministry of Economy and Competitiveness and the Xunta de Galicia have supported this work through, GRC ED431C 2020/10 and ENE2017-86425-C2-2-R projects. We are grateful to the BIOVESIN (PSE-420000-2008-4) partners for the advice and for providing us the samples of the vegetable formulated oils and the reference lubricants. Dr. María J. G. Guimarey acknowledges a postdoctoral fellowship (ED481B-2019-015) from the Xunta de Galicia (Spain) and Dr. Liñeira del Río the financial support through the Margarita Salas program (Ministry of Universities, Spain). We express our gratitude to Dr. K.R. Harris (University of New South Wales, Australia) for his high-pressure viscosity study of DiPEiC9 and also to M. A. Marcos from the University of Vigo for his help with rheology tests.

References

(1) Synthetics, Mineral Oils, and Bio-Based Lubricants: Chemistry and Technology. Chapter 42. Environmentally Friendly Hydraulic Fluids by S. Lawate; Leslie R. Rudnick, Ed.; CRC Press Taylor & Francis Group, 2020; pp 687–704.

(2) Lindemann, L. *Future Challenges of the Lubricants Industry*, *FUCHS*; 2018.

(3) Durango-Giraldo, G.; Zapata-Hernández, C.; Santa, J. F.; Buitrago-Sierra, R. Palm Oil as a Biolubricant: Literature Review of Processing Parameters and Tribological Performance. *J. Ind. Eng. Chem.* **2021**, *107*, 31–44. https://doi.org/https://doi.org/10.1016/j.jiec.2021.12.018.

(4) Willing, A. Lubricants Based on Renewable Resources – an Environmentally Compatible Alternative to Mineral Oil Products. *Chemosphere* **2001**, *43* (1), 89–98. https://doi.org/https://doi.org/10.1016/S0045-6535(00)00328-3.

(5) McNutt, J.; He, Q. S. Development of Biolubricants from Vegetable Oils via Chemical Modification. *J. Ind. Eng. Chem.* **2016**, *36*, 1–12. https://doi.org/10.1016/J.JIEC.2016.02.008.

(6) Nagendramma, P.; Kaul, S. Development of Ecofriendly/Biodegradable Lubricants: An Overview. *Renew. Sustain. Energy Rev.* **2012**, *16* (1), 764–774. https://doi.org/https://doi.org/10.1016/j.rser.2011.09.002.

(7) Mannekote, J. K.; Kailas, S. V.; Venkatesh, K.; Kathyayini, N. Environmentally Friendly Functional Fluids from Renewable and Sustainable Sources-A Review. *Renew. Sustain. Energy Rev.* **2018**, *81* (June 2016), 1787–1801. https://doi.org/10.1016/j.rser.2017.05.274.

(8) Akshai, B.; Visakh, R.; Kamath, K. J.; Riyas, M. R.; Joy, M. L. A Novel Approach in Developing Environment-Friendly Bio-Lubricant from Coconut Oil, Mustard Oil and Its Methyl Esters. *Proc. Inst. Mech. Eng. Part J J. Eng. Tribol.* **2021**, *235* (4), 765–785. https://doi.org/https://doi.org/10.1177/1350650120927170.

(9) Zainal, N. A.; Zulkifli, N. W. M.; Gulzar, M.; Masjuki, H. H. A Review on the Chemistry, Production, and Technological Potential of Bio-Based Lubricants. *Renew. Sustain. Energy Rev.* **2018**, *82*, 80–102. https://doi.org/https://doi.org/10.1016/j.rser.2017.09.004.

(10) Panchal, T. M.; Patel, A.; Chauhan, D. D.; Thomas, M.; Patel, J. V. A Methodological Review on Bio-Lubricants from Vegetable Oil Based Resources. *Renew. Sustain. Energy Rev.* **2017**, *70*, 65–70. https://doi.org/https://doi.org/10.1016/j.rser.2016.11.105.

(11) García-Zapateiro, L. A.; Franco, J. M.; Valencia, C.; Delgado, M. A.; Gallegos, C. Viscous, Thermal and Tribological Characterization of Oleic and Ricinoleic Acids-Derived Estolides and Their Blends with Vegetable Oils. *J. Ind. Eng. Chem.* **2013**, *19* (4), 1289–1298. https://doi.org/10.1016/J.JIEC.2012.12.030.

(12) Singh, R. K.; Pandey, S.; Saxena, R. C.; Thakre, G. D.; Atray, N.; Ray, S. S. Study of Cystine Schiff Base Esters as New Environmentally Benign Multifunctional Biolubricant Additives. *J. Ind. Eng. Chem.* **2015**, *26*, 149–156. https://doi.org/10.1016/J.JIEC.2014.11.027.

(13) Paredes, X.; Comuñas, M. J. P.; Pensado, A. S.; Bazile, J. P.; Boned, C.; Fernández, J. High Pressure Viscosity Characterization of Four Vegetable and Mineral Hydraulic Oils. *Ind. Crops Prod.* **2014**, *54*, 281–290. https://doi.org/10.1016/j.indcrop.2014.01.030.

(14) European Commission. Establishing the Ecological Criteria for the Award of the EU Ecolabel to Lubricants (2011/381/EU). *Off. J. Eur. Union* **2011**, *(2011) 169* (169/28), 2011/2381/EU.

(15) Martín-Alfonso, J. E.; Núñez, N.; Valencia, C.; Franco, J. M.; Díaz, M. J. Formulation of New Biodegradable Lubricating Greases Using Ethylated Cellulose Pulp as Thickener Agent. *J. Ind. Eng. Chem.* **2011**, *17* (5–6), 818–823. https://doi.org/10.1016/J.JIEC.2011.09.003.

(16) Regueira, T.; Lugo, L.; Fernández, J. Compressibilities and Viscosities of Reference, Vegetable, and Synthetic Gear Lubricants. *Ind. Eng. Chem. Res.* **2014**, *53* (11), 4499–4510. https://doi.org/10.1021/ie4034285.

(17) Kestin, J.; Wakeham, W. A.; Ho, C. Y. *Transport Properties of Fluids: Thermal Conductivity, Viscosity, and Diffusion Coefficient*; Hemisphere Pub. Corp: New York, 1988.

(18) Gaciño, F. M.; Paredes, X.; Comuñas, M. J. P.; Fernández, J. Effect of the Pressure on the Viscosities of Ionic Liquids: Experimental Values for 1-Ethyl-3-Methylimidazolium Ethylsulfate and Two Bis(Trifluoromethyl-Sulfonyl)Imide Salts. *J. Chem. Thermodyn.* **2012**, *54*, 302–309. https://doi.org/10.1016/j.jct.2012.05.007.

(19) Gaciño, F. M.; Comuñas, M. J. P.; Regueira, T.; Segovia, J. J.; Fernández, J. On the Viscosity of Two 1-Butyl-1-Methylpyrrolidinium Ionic Liquids: Effect of the Temperature and Pressure. *J. Chem. Thermodyn.* **2015**, *87*, 43–51. https://doi.org/https://doi.org/10.1016/j.jct.2015.03.002.

(20) Wakeham, W. A.; Assael, M. J.; Avelino, H. M. N. T.; Bair, S.; Baled, H. O.; Bamgbade, B. A.; Bazile, J.-P.; Caetano, F. J. P.; Comuñas, M. J. P.; Daridon, J.-L.; Diogo, J. C. F.; Enick, R. M.; Fareleira, J. M. N. A.; Fernández, J.; Oliveira, M. C.; Santos, T. V. M.; Tsolakidou, C. M. In Pursuit of a High-Temperature, High-Pressure, High-Viscosity Standard: The Case of Tris(2-Ethylhexyl) Trimellitate. *J. Chem. Eng. Data* **2017**, *62* (9), 2884–2895. https://doi.org/10.1021/acs.jced.7b00170.

(21) Caetano, F. J. P.; Fareleira, J. M. N. A.; Fröba, A. P.; Harris, K. R.; Leipertz, A.; Oliveira, C. M. B. P.; Trusler, J. P. M.; Wakeham, W. A. An Industrial Reference Fluid for Moderately High Viscosity. *J. Chem. Eng. Data* **2008**, *53* (9), 2003–2011. https://doi.org/10.1021/je800059n.

(22) Mylona, S. K.; Assael, M. J.; Comuñas, M. J. P.; Paredes, X.; Gaciño, F. M.; Fernández, J.; Bazile, J. P.; Boned, C.; Daridon, J. L.; Galliero, G.; Pauly, J.; Harris, K. R. Reference Correlations for the Density and Viscosity of Squalane from 273 to 473 K at Pressures to 200 MPa. *J. Phys. Chem. Ref. Data* **2014**, *43* (1),

13104. https://doi.org/10.1063/1.4863984.

(23) Bair, S. The Temperature and Pressure Dependence of Viscosity and Volume for Two Reference Liquids. *Lubr. Sci.* **2016**, *28* (2), 81–95. https://doi.org/https://doi.org/10.1002/ls.1302.

(24) Harris, K. R. Temperature and Pressure Dependence of the Viscosities of Krytox GPL102 Oil and Di(Pentaerythritol) Hexa(Isononanoate). *J. Chem. Eng. Data* **2015**, *60* (5), 1510–1519. https://doi.org/10.1021/acs.jced.5b00099.

(25) Fernández, J.; Assael, M. J.; Enick, R. M.; Trusler, J. P. M. International Standard for Viscosity at Temperatures up to 473 K and Pressures below 200 MPa (IUPAC Technical Report). *Pure Appl. Chem.* **2019**, *91* (1), 161–172. https://doi.org/doi:10.1515/pac-2018-0202.

(26) Harris, K. R. Correction to "Temperature and Pressure Dependence of the Viscosities of Krytox GPL102 Oil and Di(Pentaerythritol) Hexa(Isononanoate)." *J. Chem. Eng. Data* **2016**, *61* (4), 1682–1683. https://doi.org/10.1021/acs.jced.6b00114.

(27) Bair, S.; Yamaguchi, T. The Equation of State and the Temperature, Pressure, and Shear Dependence of Viscosity for a Highly Viscous Reference Liquid, Dipentaerythritol Hexaisononanoate. *J. Tribol.* **2016**, *139* (1), 011801. https://doi.org/10.1115/1.4033050.

(28) Gaciño, F. M.; Paredes, X.; Comuñas, M. J. P.; Fernández, J. Pressure Dependence on the Viscosities of 1-Butyl-2,3-Dimethylimidazolium Bis(Trifluoromethylsulfonyl)Imide and Two Tris(Pentafluoroethyl)Trifluorophosphate Based Ionic Liquids: New Measurements and Modelling. *J. Chem. Thermodyn.* **2013**, *62*, 162–169. https://doi.org/https://doi.org/10.1016/j.jct.2013.02.014.

(29) Marklund, O.; Gustafsson, L. Interferometry-Based Measurements of Oil-Film Thickness. *Proc. Inst. Mech. Eng. Part J J. Eng. Tribol.* **2001**, *215* (3), 243–259. https://doi.org/10.1243/1350650011543510.

(30) Guimarey, M. J. G.; Abdelkader, A. M.; Comuñas, M. J. P.; Alvarez-Lorenzo, C.; Thomas, B.; Fernández, J.; Hadfield, M. Comparison between Thermophysical and Tribological Properties of Two Engine Lubricant Additives: Electrochemically Exfoliated Graphene and Molybdenum Disulfide Nanoplatelets. *Nanotechnology* **2020**, *32* (2), 025701.

(31) Coelho de Sousa Marques, M. A.; Guimarey, M. J. G.; Domínguez-Arca, V.;

Amigo, A.; Fernández, J. Heat Capacity, Density, Surface Tension, and Contact Angle for Polyalphaolefins and Ester Lubricants. *Thermochim. Acta* **2021**, *703*, 178994. https://doi.org/https://doi.org/10.1016/j.tca.2021.178994.

(32) Spikes, H. A.; Hammond, C. J. The Elastohydrodynamic Film Thicknesses of Binary Ester-Ether Mixtures. *A S L E Trans.* **1981**, *24* (4), 542–548. https://doi.org/10.1080/05698198108983054.

(33) van Leeuwen, H. The Determination of the Pressure—Viscosity Coefficient of a Lubricant through an Accurate Film Thickness Formula and Accurate Film Thickness Measurements. *Proc. Inst. Mech. Eng. Part J J. Eng. Tribol.* **2009**, *223* (8), 1143–1163. https://doi.org/10.1243/13506501jet504.

(34) Bair, S.; Liu, Y.; Wang, Q. J. The Pressure-Viscosity Coefficient for Newtonian EHL Film Thickness With General Piezoviscous Response. *J. Tribol.* **2006**, *128* (3), 624–631. https://doi.org/10.1115/1.2197846.

(35) Comuñas, M. J. P.; Baylaucq, A.; Boned, C.; Fernández, J. High-Pressure Measurements of the Viscosity and Density of Two Polyethers and Two Dialkyl Carbonates at High Pressures. *Int. J. Thermophys.* **2001**, *22* (3), 749–768.

(36) Guimarey, M. J. G.; Gonçalves, D. E. P.; Liñeira del Río, J. M.; Comuñas, M. J. P.; Fernández, J.; Seabra, J. H. O. Lubricant Properties of Trimethylolpropane Trioleate Biodegradable Oil: High Pressure Density and Viscosity, Film Thickness, Stribeck Curves and Influence of Nanoadditives. *J. Mol. Liq.* **2021**, *335*, 116410. https://doi.org/https://doi.org/10.1016/j.molliq.2021.116410.

(37) Dakkach, M.; Gaciño, F. M.; Guimarey, M. J. G.; Mylona, S. K.; Paredes, X.; Comuñas, M. J. P.; Fernández, J.; Assael, M. J. Viscosity-Pressure Dependence for Nanostructured Ionic Liquids. Experimental Values for Butyltrimethylammonium and 1-Butyl-3-Methylpyridinium Bis(Trifluoromethylsulfonyl)Imide. *J. Chem. Thermodyn.* **2018**, *121*, 27–38. https://doi.org/https://doi.org/10.1016/j.jct.2018.01.025.

(38) Liñeira del Río, J. M.; Guimarey, M. J. G.; Comuñas, M. J. P.; Fernández, J. High Pressure Viscosity Behaviour of Tris(2-Ethylhexyl) Trimellitate up to 150 MPa. *J. Chem. Thermodyn.* **2019**, *138*, 159–166. https://doi.org/https://doi.org/10.1016/j.jct.2019.06.016.

(39) X. Paredes. Viscous Behaviour of Lubricants at High Pressures. Doctoral Thesis, Universidade de Santiago de Compostela, 2012.

(40) Larsson, R.; Kassfeldt, E.; Byheden, Å.; Norrby, T. Base Fluid Parameters for

Elastohydrodynamic Lubrication and Friction Calculations and Their Influence on Lubrication Capability. *J. Synth. Lubr.* **2001**, *18*, 183–198.

(41) Hamrock, B. J.; Dowson, D. *Ball Bearing Lubrication: The Elastohydrodynamic of Elliptical Contacts. Wiley/Interscience, New York*; 1981; Vol. 104. https://doi.org/10.1115/1.3253193.

(42) Bair, S.; Qureshi, F. Accurate Measurements of Pressure-Viscosity Behavior in Lubricants. *Tribol. Trans.* **2002**, *45* (3), 390–396. https://doi.org/10.1080/10402000208982564.

(43) Gupta, P. K.; Cheng, H. S.; Zhu, D.; Forster, N. H.; Schrand, J. B. Viscoelastic Effects in MIL-L-7808-Type Lubricant, Part I: Analytical Formulation. *Tribol. Trans.* **1992**, *35* (2), 269–274. https://doi.org/10.1080/10402009208982117.

(44) Cheng, H. S. A Refined Solution to the Thermal-Elastohydrodynamic Lubrication of Rolling and Sliding Cylinders. *A S L E Trans.* **1965**, *8* (4), 397–410. https://doi.org/10.1080/05698196508972110.

(45) Wilson, W. R. D.; Sheu, S. Effect of Inlet Shear Heating Due To Sliding on Elastohydrodynamic Film Thickness. *J. Lubr. Technol.* **1983**, *105* (2), 187–188. https://doi.org/10.1115/1.3254563.

(46) Rojas, E.; Coimbra, J.; TelisRomero, J. Thermophysical Properties of Cotton, Canola, Sunflower and Soybean Oils as a Function of Temperature. *Int. J. Food Prop.* **2013**, *16*, 1620. https://doi.org/10.1080/10942912.2011.604889.

(47) Gomna, A.; N'Tsoukpoe, K. E.; Le Pierrès, N.; Coulibaly, Y. Review of Vegetable Oils Behaviour at High Temperature for Solar Plants: Stability, Properties and Current Applications. *Sol. Energy Mater. Sol. Cells* **2019**, *200*, 109956. https://doi.org/10.1016/J.SOLMAT.2019.109956.

(48) Zhu, D.; Wang, J.; Jane Wang, Q. On the Stribeck Curves for Lubricated Counterformal Contacts of Rough Surfaces. *J. Tribol.* **2015**, *137* (2). https://doi.org/10.1115/1.4028881.

(49) Gonçalves, D.; Vieira, A.; Carneiro, A.; Campos, A. V; Seabra, J. H. O. Film Thickness and Friction Relationship in Grease Lubricated Rough Contacts. *Lubricants* **2017**, *5* (3), 34. https://doi.org/10.3390/lubricants5030034.

(50) Keller, A. A.; Broje, V.; Setty, K. Effect of Advancing Velocity and Fluid Viscosity on the Dynamic Contact Angle of Petroleum Hydrocarbons. *J. Pet. Sci. Eng.* **2007**, *58* (1), 201–206. https://doi.org/https://doi.org/10.1016/j.petrol.2006.12.002.

(51) Zitzenbacher, G.; Dirnberger, H.; Längauer, M.; Holzer, C. Calculation of the Contact Angle of Polymer Melts on Tool Surfaces from Viscosity Parameters. *Polymers (Basel).* **2018**, *10* (1), 38. https://doi.org/10.3390/polym10010038.

Table 1. Physical properties of the specimens used for film thickness and friction coefficient measurements.

Property	Ball	Glass disc	Steel disc		
			SD1	SD2	SD3
Elastic modulus E / GPa	210	64	207	207	207
Poisson coefficient υ / GPa	0.29	0.20	0.29	0.29	0.29
Radius R / mm	9.52	50	50	50	50
Surface roughness σ/ nm	20	5	100	200	500

Table 2. Dynamic viscosities, η/mPa s, obtained with the Anton Paar Stabinger SVM3000 for BIO-G00 and BIO-G02 at atmospheric pressure.

T / K	BIO-G00	BIO-G02
288.15	1018	544.1
293.15	723.5	397.7
298.15	526.2	296.5
303.15	390.7	225.3
308.15	295.5	174.3
313.15	227.5	136.9
318.15	178.0	109.2
323.15	141.3	88.34
328.15	113.8	72.36
333.15	92.81	59.96
338.15	76.60	50.24
343.15	63.91	42.51
348.15	53.88	36.31
353.15	45.85	31.27
358.15	39.33	27.15
363.15	34.03	23.74
368.15	29.66	20.90
373.15	26.02	18.52

Expanded uncertainties (k=2) are $U(T)$ = ±0.02 K, $U(p)$ = ±0.0005 MPa and $U_r(\eta)$ = 1%.

Table 3. Dynamic viscosity as a function of pressure, η/mPa·s, for the formulated vegetable oils under study.

T/K	*p/MPa*	η/mPa·s	*T*/K	*p/MPa*	η/mPa·s
		BIO-G00			
313.15	10	252.3	343.15	125	450.5
313.15	25	392.9	343.15	150	610.2
313.15	50	712.3	343.15	175	813.9
313.15	75	1156	343.15	200	1074
313.15	100	1758	343.15	225	1407
313.15	125	2573	343.15	250	1835
313.15	150	3684	363.15	125	188.8
313.15	175	5215	363.15	150	257.1
313.15	200	7351	363.15	175	334.1
313.15	225	10370	363.15	200	419.7
313.15	250	14720	363.15	225	514.9
343.15	75	228.4	363.15	250	621.1
343.15	100	325.6			
		BIO-G02			
313.15	10	179.5	343.15	100	199.8
313.15	25	260.3	343.15	125	274.4
313.15	50	435.5	343.15	150	367.9
313.15	75	669.4	343.15	175	484.6
313.15	100	977.6	343.15	200	630.5
313.15	125	1385	343.15	225	813.4
313.15	150	1930	343.15	250	1043
313.15	175	2666	363.15	175	212.3
313.15	200	3676	363.15	200	260.8
313.15	225	5083	363.15	225	318.3
313.15	250	7072	363.15	250	385.1

Expanded uncertainties (k=2) are $U(T)$ = ±0.1 K, $U(p)$ = ±0.2 MPa and $U_r(\eta)$ = 5%.

Table 4. Viscosity correlation parameters, equation (5) and (6).

	BIO-G00	BIO-G02
A·/ mPa·s	0.07820 ± 0.00406	0.08726 ± 0.00414
B / K	1262.4 ± 15.4	1166.45 ± 14.2
C / K	154.92 ± 0.90	154.66 ± 0.91
D	4.8062 ± 0.5125	4.1104 ± 0.4649
E_0 / MPa	599.22 ± 4.19	507.33 ± 6.09
E_1 / MPa·K^{-1}	-4.3506 ± 0.087	-3.6547 ± 0.109
10^3 E_2·/ MPa·K^{-2}	9.70405 ± 0.00065	8.15944 ± 0.00045
AAD / %	3.0	2.7

Table 5. Universal pressure-viscosity coefficient (α_{film}) and reciprocal asymptotic isoviscous pressure coefficient (α^*).

T/K	α_{film} / GPa^{-1}	$\alpha*$/GPa^{-1}
	BIO-G00	
313.15	21.5	20.2
343.15	16.3	15.3
363.15	13.6	12.8
	BIO-G02	
313.15	20.7	19.1
343.15	15.7	14.6
363.15	13.2	12.2

Table 6. Contact angles (θ) and their uncertainties (σ).

T / K	θ/°	σ/°	θ/°	σ/°
	BIO-G00		BIO-G02	
303.15	32.4	1.2	18.0	1.4
323.15	12.3	1.2	14.3	0.9
353.15	9.2	1.2	11.1	1.1